International Journal of Applied Mathematics
Volume 25 No. 6 2012, 883-908

NUMERICAL STUDY OF AN UNSTEADY 2-D INCOMPRESSIBLE VISCOUS FLOW WITH HEAT TRANSFER AT MODERATE REYNOLDS NUMBER WITH SLIP BOUNDARY CONDITIONS

V. Ambethkar[1] §, Mohit Kumar Srivastava[2]
[1,2]Department of Mathematics
Faculty of Mathematical Sciences
University of Delhi
Delhi, 110007, INDIA
[1]e-mails: vambethkar@maths.du.ac.in, vambethkar@gmail.com
[2]e-mail: srivastava264@gmail.com

Abstract: In this present study the problem of an unsteady 2-D incompressible viscous flow with heat transfer at moderate Reynolds number with slip boundary conditions was investigated. Numerical solutions of the governing equations are obtained by using the marker and cell (MAC) method of pressure correction approach. The numerical computations for u-velocity, v-velocity, pressure and temperature have been conducted using an efficient solver based on staggered grid system. The numerical computations for u-velocity, v-velocity, pressure and temperature at different times for different positions along ox and oy have been computed. The numerical solutions of the u-velocity, v-velocity, pressure and temperature obtained in this present study have been ensured to be stable based on the stability requirements obtained for the present solver. The significant findings from this present investigation have been given under conclusion.

Received: December 29, 2012

§Correspondence author

AMS Subject Classification: 35Q30, 76D05, 76M20, 80A20
Key Words: heat transfer, Navier-Stokes equations, Marker-And-Cell (MAC) method, primitive variables, Reynolds number, slip boundary conditions

1. Introduction

Unsteady 2-D incompressible viscous flow with heat transfer is a complex problem of great practical significance.The study of fluid flow and heat transfer has received considerable attention because of numerous thermal engineering in various disciplines, such as geothermal extraction, storage of radioactive nuclear waste materials, transfer ground water pollution, oil recovery processes, geophysical thermal insulation, cooling of electronic components, food processing, casting and welding of manufacturing processes and the dispersion of chemical contaminants in various processes in the chemical industry. Heat transfer has broad application to the functioning of numerous devices and systems. Heat-transfer principles may be used to preserve, increase, or decrease temperature in a wide variety of circumstances.Reynolds numbers frequently arise when performing dimensional analysis of fluid dynamics problems, and as such can be used to determine dynamic similitude between different experimental cases. They are also used to characterize different flow regimes, such as laminar or turbulent flow.

Harlow and Welch [1] used the marker and cell (MAC) method for numerical calculation of time-dependent viscous incompressible flow of fluid with free surface. This method is restricted to staggered grid. Toru Fusegi and Bakitter Farouk [4] gave relatively novel formulation of the Navier-Stokes equations is evaluated for obtaining solutions of l-dimensional incompressible fluid flow and convective heat transfer problems. A vorticity transport equation along with two Poisson equations for the velocity components and the energy equation are solved by a finite difference scheme. Flow and heat transfer of a participating medium over a right circular cylinder was investigated experimently and numerically by D.A. Kaminiski, X.D. Fu, M.K. Jensen [5]. A finite-element method was used to solve low Reynolds number flow over a circular cylinder in a radiatively participating medium. Maksym Grzywinski, Andrzej Sluzalec [7] solved the Stochastic convective heat transfer equations in finite differences method. A numerical procedure based on the stochastic finite differences method was developed for the analysis of general problems in free/forced convection heat transfer. The discretization of the field equations through use of the finite differences approximation method was described. One-dimensional

axisymmetrical problem was solved as an example. N.T. Eldabe et al [8] investigated the problem of heat transfer to MHD flow of a micropolar fluid from a stretching sheet with suction and blowing through a porous medium is studied numerically by using Chebyshev finite difference method (ChFD). A similarity solution to governing momentum, angular momentum and energy equations is derived. The effects of surface mass transfer, Prandtl number, magnetic field and porous medium on the velocities and temperature profiles have been studied. In Arnab Kumar De and Amaresh Dalal [9] natural convection around a tilted heated square cylinder kept in an enclosure has been studied in the range of $1000 \leq Ra \leq 100000$. Detailed flow and heat transfer features for two different thermal boundary conditions are reported. P.H. Chiu et al [10] proposed an effective explicit pressure gradient scheme implemented in the two-level non-staggered grids for incompressible Navier–Stokes equations. An improved two-level method was presented for effectively solving the incompressible Navier–Stokes equations. This proposed method solves a smaller system of nonlinear Navier–Stokes equations on the coarse mesh. Tomasz Piasecki [12] examined a steady flow of compressible fluid with inflow boundary condition on the density and slip boundary conditions on the velocity in a square domain. Qiaolin He and Xiao-Ping Wang [13] studied the driven cavity flow using the Navier slip boundary condition. The results have shown that the Navier slip boundary condition removes the corner singularity induced by the no-slip boundary condition. The behaviour of the tangential stress is examined and the results are obtained for low Reynolds number. A.A. Lambert et al [14] studied the heat transfer enhancement in oscillatory flows of Newtonian and viscoelastic fluids. Saleh M. Alharbi et al [15] presented the study of convective heat and mass transfer characteristics of an incompressible MHD visco-elastic fluid flow immersed in a porous medium over a stretching sheet with chemical reaction and thermal stratification effects. The resultant governing boundary layer equations are highly non-linear and coupled form of partial differential equations, and they have been solved by using fourth order Runge-Kutta integration scheme with Newton Raphson shooting method. Tiegang Fang et al [17] investigated the steady momentum and heat transfer of a viscous fluid flow over a stretching/shrinking sheet. Exact solutions are presented for the Navier–Stokes equations.

The new solutions provide a more general formulation including the linearly stretching and shrinking wall problems as well as the asymptotic suction velocity profiles over a moving plate. B.H. Salman et al [18] solved. The governing (continuity, momentum and energy) equations using the finite volume method (FVM) with the aid of SIMPLE algorithm. This investigation covers Reynolds

number in the range of 10 to 1500. Asma Begum et al [19] studied the finite difference analysis of natural convection flow over an inclined plate numerically namely implicit finite-difference method of Crank-Nicolson type. M. Hasanuzzaman et al [20] investigated the effects of Lewis number on heat and mass transfer in a triangular cavity. The double-diffusive mixed convection in a right triangular is analyzed by solving the mass, momentum, energy and concentration balance equations. The flow is considered to operate in the laminar regime under steady state conditions.

In view of the available literature mentioned above on the problem of an unsteady 2-D incompressible viscous flow with heat transfer at moderate Reynolds number with slip boundary conditions has not been studied widely by the researchers due to the complexity involved in computing four unknown variables u, v, p, T simultaneously. Especially in case of moderate Reynolds number flow with slip boundary conditions, the computational procedure though tedious, it is powerful and efficient one which gives a stable solution. Moreover, in this type of problem the physical domain is a rectangular cavity for which calculation procedure becomes more complicated due to different step length of the computational grid.

Due to the reasons mentioned in the above para, we have been motivated by the present investigation. It solves an unsteady 2-D incompressible viscous flow with heat transfer at moderate Reynolds number with slip boundary conditions with marker and cell (MAC) method of pressure correction approach. The study was conducted using an efficient solver based on staggered grid system. The stability of the numerical solutions of velocity in x and y direction, pressure and temperature has been ensured.

2. Mathematical Formulation

We consider an unsteady 2-D incompressible viscous flow with heat transfer at moderate Reynolds number with slip boundary conditions. Let this flow passes through a rectangular cavity as described in Figure 1. All fluid properties are assumed to be constant. Except the influence of density variation with temperature is consider only in the body force term. Under these assumption and taking the usual Boussinesq approximations into account the governing equations for 2-D incompressible viscous Navier-stokes equations in dimensionless

form are given by:

$$\text{Continuity Equation} \quad \frac{\partial u}{\partial x}+\frac{\partial v}{\partial y}=0, \tag{1}$$

$$\text{X-Momentum} \quad \frac{\partial u}{\partial t}+u\frac{\partial u}{\partial x}+v\frac{\partial u}{\partial y}=-\frac{\partial P}{\partial x}+\left(\frac{1}{R_e}\right)\left(\frac{\partial^2 u}{\partial x^2}+\frac{\partial^2 u}{\partial y^2}\right), \tag{2}$$

$$\text{Y-Momentum} \quad \frac{\partial v}{\partial t}+u\frac{\partial v}{\partial x}+v\frac{\partial v}{\partial y}=-\frac{\partial P}{\partial y}+\left(\frac{1}{R_e}\right)\left(\frac{\partial^2 v}{\partial x^2}+\frac{\partial^2 v}{\partial y^2}\right), \tag{3}$$

$$\text{Energy Equation} \quad \frac{\partial T}{\partial t}+u\frac{\partial T}{\partial x}+v\frac{\partial T}{\partial y}=K\left(\frac{\partial^2 T}{\partial x^2}+\frac{\partial^2 T}{\partial y^2}\right), \tag{4}$$

with the following initial and boundary conditions:

$$\text{For } t=0: \quad u(x,y,0)=0,\ v(x,y,0)=0,\ T(x,y,0)=0, \tag{5}$$

$$\begin{aligned} &\text{For } t>0: \\ &\text{At wall } AB: \quad x=0 \text{ and } 0\le y\le 1,\ v=0.5,\ T=0.5, \\ &\text{At wall } BC: \quad y=0 \text{ and } 0\le x\le 2,\ u=1,\ T=1 \\ &\text{At wall } CD: \quad x=2 \text{ and } 0\le y\le 1,\ v=0.5,\ T=0.5 \\ &\text{At wall } AD: \quad y=1 \text{ and } 0\le x\le 2,\ u=1,\ T=1 \end{aligned} \tag{6}$$

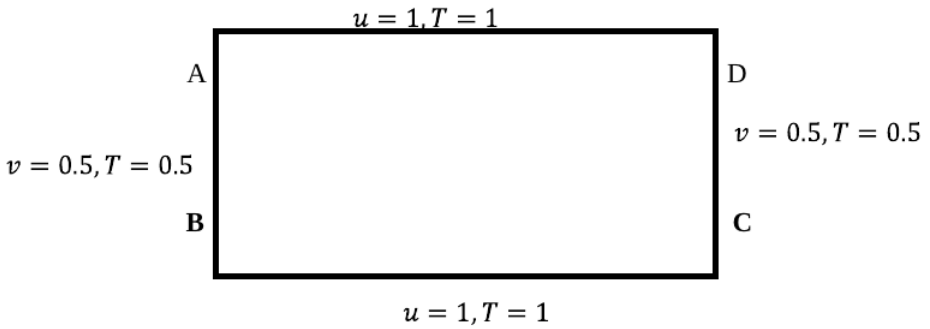

Figure 1: Rectangular cavity

3. Method of Solution

In order to solve the equations (1)-(3) which are semi-linear coupled partial differential equations we use marker and cell (MAC) method of Harlow and

Welch [1]. Considering the P, $u$and v nodes in the MAC configuration (Figure 2), the x-momentum equation is written at the u nodes, and the y-momentum equation is written at the v nodes. Accordingly, the various derivatives in the x-momentum equation (2) are calculated as follows:

$$\left(\frac{\partial u}{\partial t}\right)^{n+1}_{i+1/2,j} = (u^{n+1}_{i+1/2,j} - u^{n}_{i+1/2,j})/\Delta t, \tag{7}$$

$$\left(\frac{\partial P}{\partial x}\right)^{n+1}_{i+1/2,j} = (P^{n+1}_{i+1,j} - P^{n+1}_{i,j})/\Delta x. \tag{8}$$

Using the MAC method, the other terms in the X-momentum equation (2) are written as

$$\left(u\frac{\partial u}{\partial x}\right)^{n}_{i+1/2,j} = u^{n}_{i+1/2,j}(u^{n}_{i+3/2,j} - u^{n}_{i-1/2,j})/2\Delta x, \tag{9}$$

$$\left(v\frac{\partial u}{\partial y}\right)^{n}_{i+1/2,j} = v^{n}_{i+1/2,j}(u^{n}_{i+1/2,j+1} - u^{n}_{i+1/2,j-1})/2\Delta y. \tag{10}$$

Here $v^{n}_{i+1/2,j}$ is given by

$$v^{n}_{i+1/2,j} = (v^{n}_{i,j+1/2} + v^{n}_{i,j-1/2} + v^{n}_{i+1,j+1/2} + v^{n}_{i+1,j-1/2})/4. \tag{11}$$

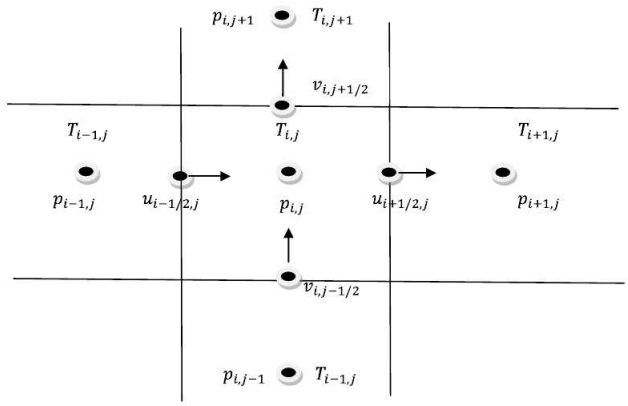

Figure 2: MAC staggered grid system

For simplicity, we will implement a fully explicit version of the time-splitting (fractional time-step) method, for both the viscous and the diffusion terms.

When this method is applied to the x-momentum equation on the staggered grid from time level t to $\hat{t}$ yields the following equation at the intermediate step:

$$\frac{\hat{u}_{i+1/2,j} - u^n_{i+1/2,j}}{\Delta t} = u^n_{i+1/2,j}\frac{(u^n_{i-1/2,j} - u^n_{i+3/2,j})}{2\Delta x} + v^n_{i+1/2,j}\frac{(u^n_{i+1/2,j-1} - u^n_{i+1/2,j+1})}{2\Delta y} + \frac{u^n_{i+3/2,j} - 2u^n_{i+1/2,j} + u^n_{i-1/2,j}}{R_e\Delta x^2} + \frac{u^n_{i+1/2,j+1} - 2u^n_{i+1/2,j} + u^n_{i+1/2,j-1}}{R_e\Delta y^2}. \quad (12)$$

Similarly for the y-momentum equation we obtain the following equation:

$$\frac{\hat{v}_{i,j+1/2} - v^n_{i,j+1/2}}{\Delta t} = u^n_{i,j+1/2}\frac{v^n_{i-1,j+1/2} - v^n_{i+1,j+1/2}}{2\Delta x} + v^n_{i,j+1/2}\frac{v^n_{i,j-1/2} - v^n_{i,j+3/2}}{2\Delta y} + \frac{v^n_{i+1,j+1/2} - 2v^n_{i,j+1/2} + v^n_{i-1,j+1/2}}{R_e\Delta x^2} + \frac{v^n_{i,j+3/2} - 2v^n_{i,j+1/2} + v^n_{i,j-1/2}}{R_e\Delta y^2}. \quad (13)$$

Practical stability requirement obtained from the Von Neumann analysis for the Euler explicit solver are given by Peyret and Taylor [3, 148] as follows:

$$(|u| + |v|)^2\Delta t Re \leq 4, \quad (14)$$

$$\frac{\Delta t}{\mathrm{Re}}[\frac{1}{\Delta x^2} + \frac{1}{\Delta y^2}] \leq 5, \quad (15)$$

$$\Delta t^{\max}_{i,j}[\left(\frac{u_{i,j}}{\Delta x} + \frac{v_{i,j}}{\Delta y}\right)\frac{1}{R_e} + 2K(\frac{1}{\Delta x^2} + \frac{1}{\Delta y^2})] \leq 1. \quad (16)$$

Now advancing from t^n to $\hat{t}$ and then $\hat{t}$ to t^{n+1} one obtains the elliptical pressure equation:

$$\frac{\nabla.\hat{U}}{\Delta t} = \nabla^2 P^{n+1}. \quad (17)$$

Pressure boundary conditions are all homogeneous Neumann boundary conditions, given by $\frac{\partial p^{n+1}}{\partial n} = 0$, now using central difference scheme:

$$\frac{P^{n+1}_{i+1,j} - 2P^{n+1}_{i,j} + P^{n+1}_{i-1,j}}{\Delta x^2} + \frac{P^{n+1}_{i,j+1} - 2P^{n+1}_{i,j} + P^{n+1}_{i,j-1}}{\Delta y^2} = \frac{1}{\Delta t}\left[\frac{\hat{u}_{i+1/2,j} - \hat{u}_{i-1/2,j}}{\Delta x} + \frac{\hat{v}_{i,j-1/2} - \hat{v}_{i,j-1/2}}{\Delta y}\right]. \quad (18)$$

We obtain the velocity field at the advanced time level $(n+1)$, for each velocity component, this equation gives

$$u_{i+1/2,j}^{n+1} = \hat{u}_{i+1/2,j} - \frac{\Delta t}{\Delta x}(P_{i+1,j}^{n+1} - P_{i,j}^{n+1}), \tag{19}$$

$$v_{i,j+1/2}^{n+1} = \hat{v}_{i,j+1/2} - \frac{\Delta t}{\Delta y}(P_{i,j+1}^{n+1} - P_{i,j}^{n+1}). \tag{20}$$

For the heat transfer equation

$$\frac{T_{i,j}^{n+1} - T_{i,j}^{n}}{\Delta t} = u_{i,j}^{n}\frac{T_{i-1,j}^{n} - T_{i+1,j}^{n}}{\Delta x} + v_{i,j}^{n}\frac{T_{i,j-1}^{n} - T_{i,j+1}^{n}}{\Delta y} + K\frac{T_{i+1,j}^{n} - 2T_{i,j}^{n} + T_{i-1,j}^{n}}{\Delta x^2} + K\frac{T_{i,j+1}^{n} - 2T_{i,j}^{n} + T_{i,j-1}^{n}}{\Delta y^2}. \tag{21}$$

But we note that $u_{i,j}^{n}$ is not defined on a u node and $v_{i,j}^{n}$ so that to obtain this quantity, we use averaging such that

$$u_{i,j}^{n} = \frac{1}{2}\left(u_{i+1/2,j}^{n} + u_{i-1/2,j}^{n}\right) \text{ and } v_{i,j}^{n} = \frac{1}{2}\left(v_{i,j+1/2}^{n} + v_{i,j-1/2}^{n}\right).$$

4. Numerical Computations

In the numerical computation for the finding the unknown velocity and pressure a rectangular staggered computational grid has been used which has been described under Figure 3. This grid has been taken in connection with the physical significance of the problem. The boundary conditions on the rectangular staggered grid are in view of the present physical problem under investigation. Initially at the start of the computation for $t = 0$, we have u-velocity and v-velocity and Temperature to be zero. The u–velocity,v-velocity and pressure have been then computed by time marching method with a time difference of $\Delta t = 0.0005$.

4.1. Summary of a Calculation Step

The fluid flow of a nonhomogeneous and nonisothermal fluid under the Bossiness approximation is numerically advanced by a sequence of computational steps, each of finite length Δt.

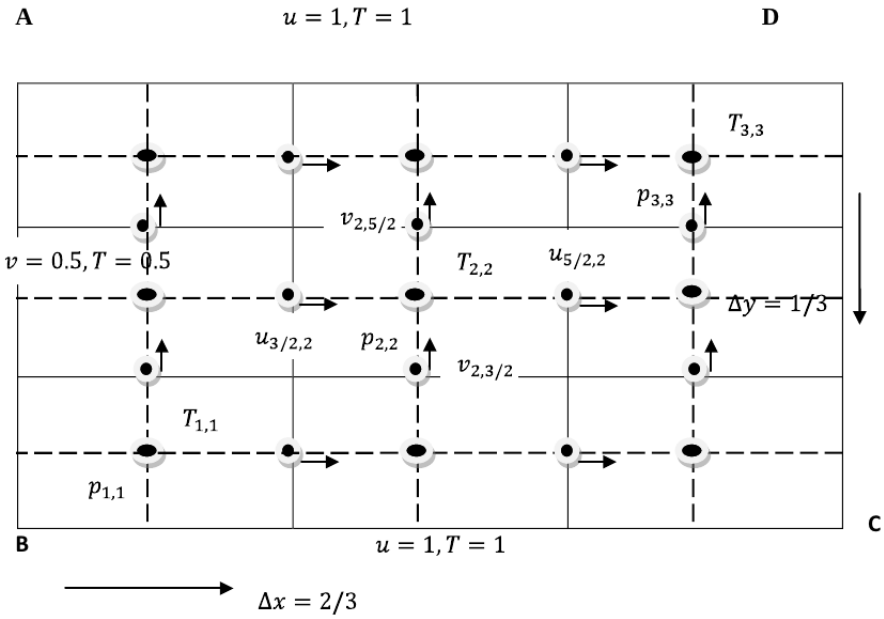

Figure 3: The rectangular staggered computational grid

4.1.1. Prediction Step

- Using (12) and (13), calculate $\hat{u}$ and $\hat{v}$ at their respective grid point locations.
- Apply the boundary conditions.
- Linear stability conditions (14),(15) and (16) must be obeyed.
- Divergence of the velocity field must be calculated at every time step, using the velocity field at the advanced time level, $(n+1)$

$$\nabla \mathbf{u} = \frac{u^{n+1}_{i+1/2,j} - u^{n+1}_{i-1/2,j}}{\Delta x} + \frac{v^{n+1}_{i,j+1/2} - v^{n+1}_{i,j-1/2}}{\Delta y}.$$

The sum of the divergence magnitude at all grid points should be satisfied to machine zero at each time step. If this quantity increases, the calculation should be terminated and restarted with a smaller time step.

4.1.2. Pressure Calculation

- Calculate pressure from Pressure-Poisson equation (17).
- Boundary condition applied to the pressure equation at all boundaries is the homogeneous Neumann boundary conditions. This equation is solved at the pressure (ij). Note that the Euler explicit time-advancement calculates the actual thermodynamic pressure (scaled by the constant density) and not a pseudo-pressure.

4.1.3. Velocity Correction

- Obtain the velocity field at the advanced time level $(n+1)$, for each velocity component, this equation gives

$$u_{i+1/2,j}^{n+1} = \hat{u}_{i+1/2,j} - \frac{\Delta t}{\Delta x}(P_{i+1,j}^{n+1} - P_{i,j}^{n+1}),$$

$$v_{i,j+1/2}^{n+1} = \hat{v}_{i,j+1/2} - \frac{\Delta t}{\Delta y}(P_{i,j+1}^{n+1} - P_{i,j}^{n+1}).$$

4.1.4. Temperature Calculation

- Determine of the temperature $T_{i,j}^{n}$ by an explicit calculation with the finite difference equation (21) and (22).

5. Results and Disscussion

In order to get clear inside in to the problem numerical computations are carried out for different times and are displayed. While doing the computations for unknown variables like u (x-component of velocity), v (y-component of velocity), p (pressure) and T (temperature), the Reynolds number (Re) has been chosen to be 5000, $K = 1$, $\Delta t = 0.0005$, $\Delta x = 2/3$, $\Delta y = 1/3$. While computing u-velocity, $v$velocity, pressure and temperature by following a method which has been described under Section 3. This method has been summarized under an algorithm given under Section 4.1. The same algorithm has been implemented in C-programming language. The unknown quantities velocity of the fluid flow in x and y directions, the pressure and temperature which have

been described under Tables 1 to 4. The u-velocity at different times 0.001, 0.002, 0.003, 0.004, 0.005 with different positions along ox and oy have been computed and described under Table 1. Similarly the v-velocity at different times described above along ox and oy has been computed and described under Table 2. Finally numerical solutions for pressure and temperature at different times 0.001, 0.002, 0.003, 0.004, 0.005 have been computed and described under Table 3 and Table 4.

x	y	u(t = .001)	u(t = .002)	u(t = .003)	u(t = .004)	u(t = .005)
0.6667	0.3334	0.000001	0.000001	0.000002	0.000002	0.000002
1.3334	0.3334	0.000001	0.000002	0.000003	0.000003	0.000003
0.6667	0.6667	-0.000002	-0.000003	-0.000004	-0.000005	-0.000005
1.3334	0.6667	-0.000002	-0.000003	-0.000004	-0.000005	-0.000005
0.6667	1.0000	0.000001	0.000002	0.000002	0.000003	0.000003
1.3334	1.0000	0.000001	0.000001	0.000002	0.000002	0.000002

Table 1: Numerical solutions of u-velocity

The u-velocity of the fluid at different times 0.001, 0.002, 0.003, 0.004, 0.005 is illustrated in Figures 4 to 8. The u-velocity at different positions (0.6667, 1.3334) along the ox but at different times 0.001, 0.002, 0.003, 0.004, 0.005 have been illustrated in Figure 9 and Figure 10. The u-velocity of the fluid at t =0.001 and at different positions along x-axis (0.6667, 1.3334) for which the position on y-axis at 0.1667 and 1.0 has been observed from Figure 4. It can be seen that the velocity along x-axis (u-velocity) increases steadily. But u-velocity at time t =0.001 for different positions along x-axis 0.6667, 1.3334 for which the position on y-axis at 0.6667 decreases steadily. Same behavior of u-velocity of the fluid is observed in Figures 5 to 8. The behavior of the u-velocity of the fluid at different times and different positions along x-axis has been illustrated from Figure 9 and Figure 10. In this case it has been observed how the numerical solution of u-velocity varies at different instants of time. Physically it has been observed that the u-velocity for y =0.3334 and y =1.0 increases as time passes at a particular position on x-axis. For y =0.6667 at particular position on x-axis the u-velocity decreases as time passes. In other words we can say that the absolute value of the u-velocity increases as time passes for different positions on oy

The v-velocity of the fluid at different times 0.001, 0.002, 0.003, 0.004, 0.005 is illustrated in Figures 11 to 15. From Figures 11 to 15 it has been observed that for y =0.3334 at a particular time the v-velocity increases for increase in the value of x. Also it has been observed that for y =0.6667 at a particular time the v-velocity decreases with increase in the value of xThe v-velocity at

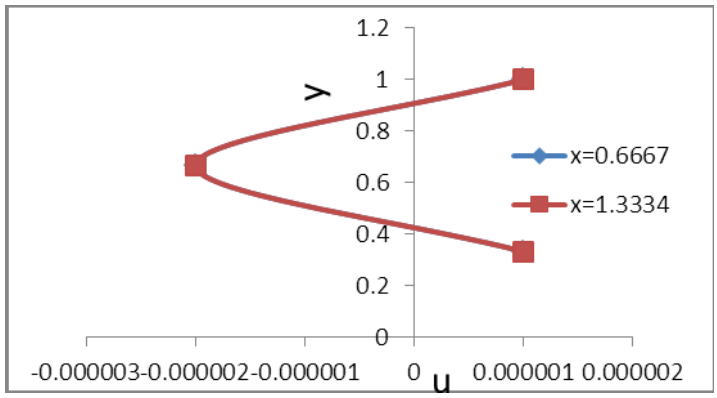

Figure 4: u-velocity at t=0.001

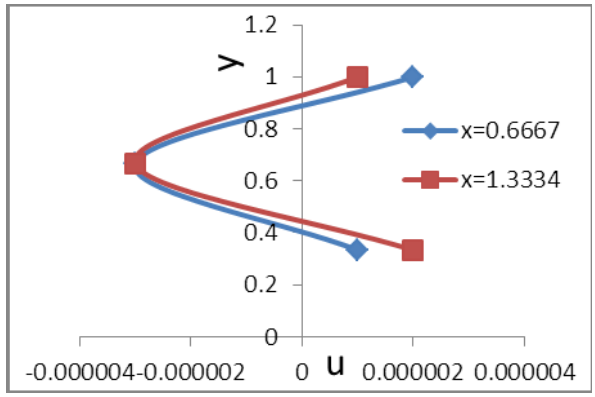

Figure 5: u-velocity at t=0.002

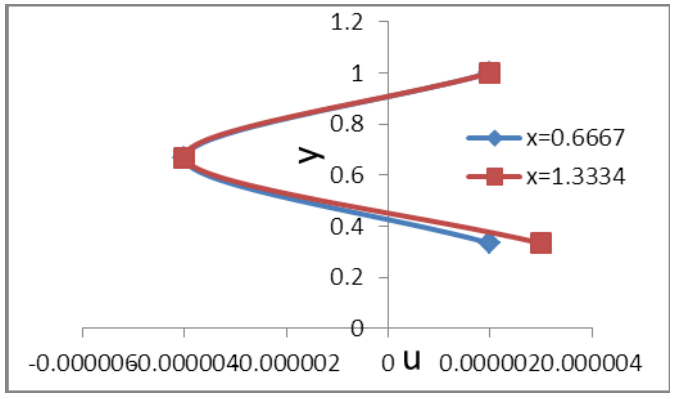

Figure 6: u-velocity at t=0.003

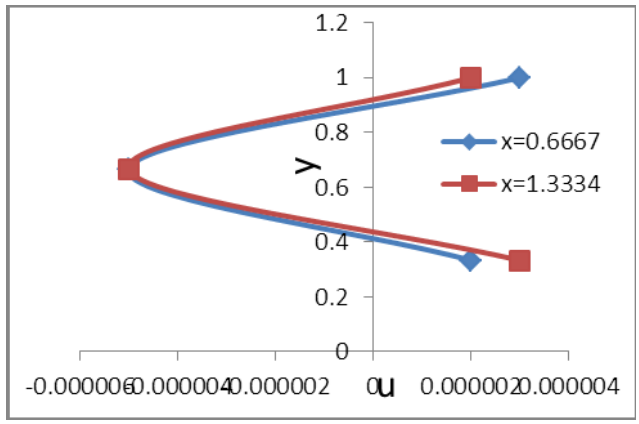

Figure 7: u-velocity at t=0.004

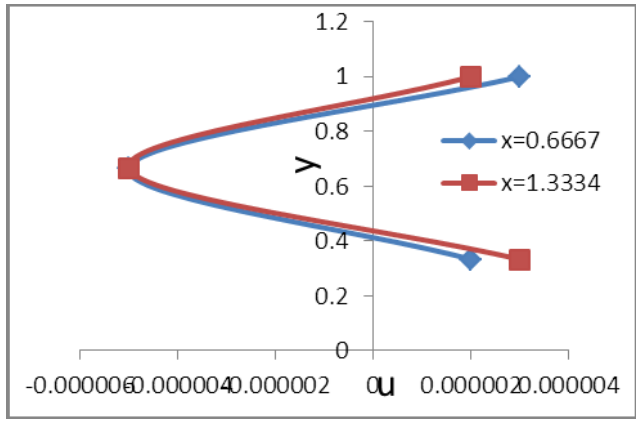

Figure 8: u-velocity at t=0.005

x	y	v(t = .001)	v(t = .002)	v(t = .003)	v(t = .004)	v(t = .005)
0.3334	0.3334	-0.000001	-0.000001	-0.000002	-0.000002	-0.000002
0.3334	0.6667	0.000001	0.000001	0.000001	0.000001	0.000001
1.0000	0.3334	0.000000	0.000000	0.000000	0.000000	0.000000
1.0000	0.6667	0.000000	0.000000	0.000000	0.000000	0.000000
1.6667	0.3334	0.000001	0.000001	0.000001	0.000001	0.000001
1.6667	0.6667	-0.000001	-0.000001	-0.000002	-0.000002	-0.000002

Table 2: Numerical solutions of v-velocity

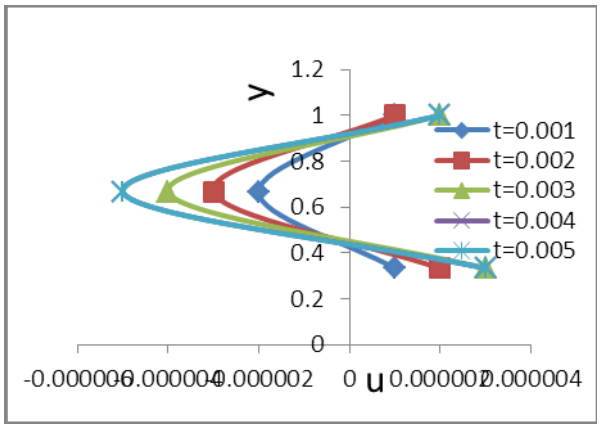

Figure 9: u-velocity at x=0.6667

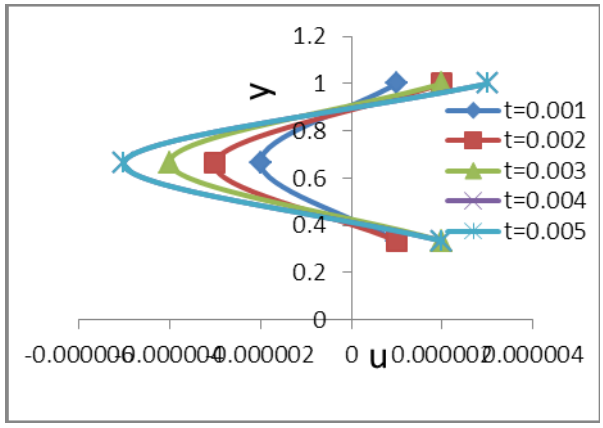

Figure 10: u-velocity at x=1.3334

different positions (0.3334, 0.6667) along oy but at different times 0.001, 0.002, 0.003, 0.004, 0.005, have been illustrated in Figure 16 and Figure 17. From Figure 16 it can be observed that for y =0.3334 the v-velocity increases with increase in the value of x. This increase in v-velocity is more rapid as time increase from t =0.001 to t =0.004 and it is convergent thereafter. Exactly a reverse behavior of v-velocity has been observed from Figure 17.

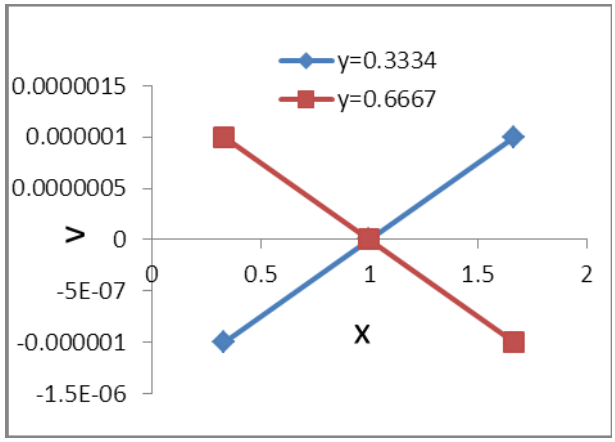

Figure 11: v-velocity at t=0.001

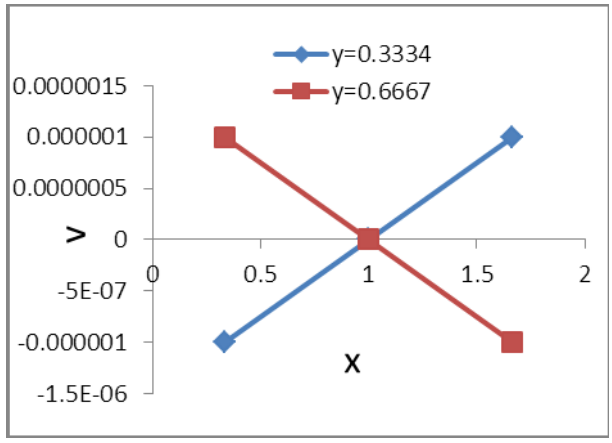

Figure 12: v-velocity at t=0.002

The numerical solutions for the pressure at different times 0.001, 0.002, 0.003, 0.004, 0.005 for given values of x and y which varies from 0.0 to 2.0 and 0.0 to 1.0 respectively have been computed and given in Table 3. The pressure

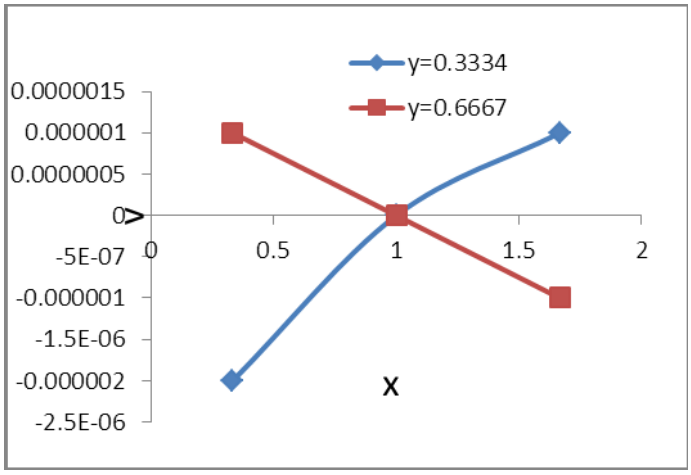

Figure 13: v-velocity at t=0.003

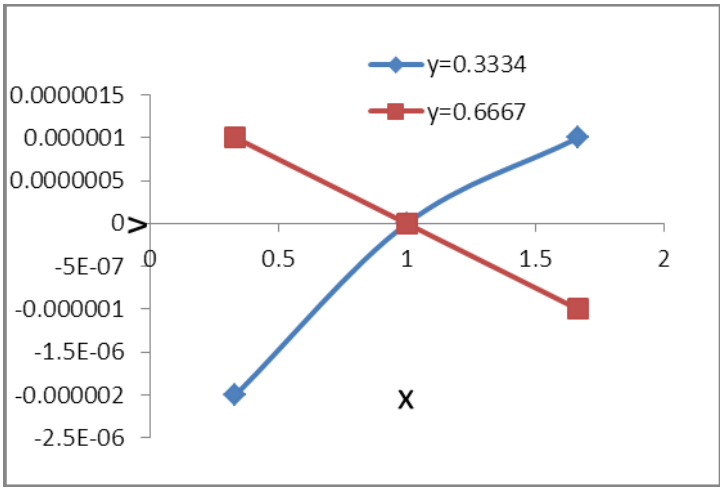

Figure 14: v-velocity at t=0.004

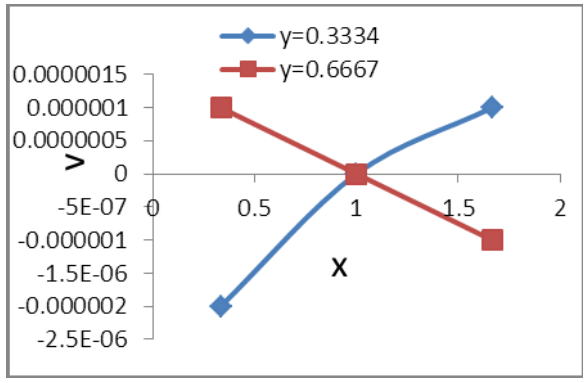

Figure 15: v-velocity at t=0.005

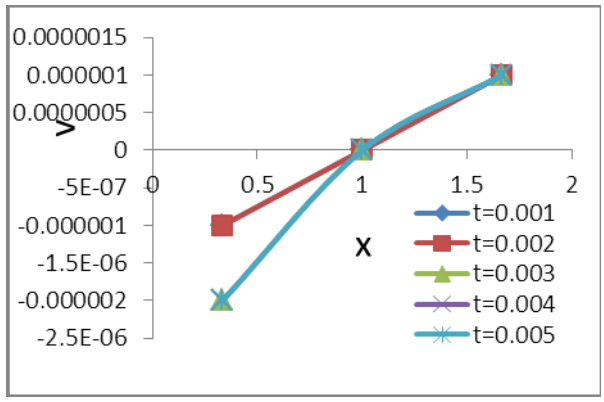

Figure 16: v-velocity at y=0.3334

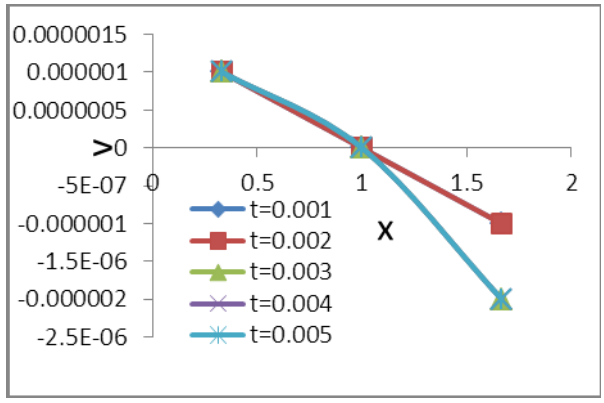

Figure 17: v-velocity at y=0.6667

x	y	p(t = .001)	p(t = .002)	p(t = .003)	p(t = .004)	p(t = .005)
0.3334	0.1667	0.0000	0.0000	0.0000	0.0000	0.0000
1.0000	0.1667	0.0015	0.0013	0.0011	0.0010	0.0010
1.6667	0.1667	0.0037	0.0039	0.0041	0.0042	0.0043
0.3334	0.3334	0.0001	0.0001	0.0001	0.0001	0.0001
1.0000	0.3334	0.0017	0.0015	0.0014	0.0013	0.0013
1.6667	0.3334	0.0037	0.0039	0.0041	0.0042	0.0043
0.3334	0.6667	0.0002	0.0002	0.0001	0.0001	0.0001
1.0000	0.6667	0.0018	0.0015	0.0013	0.0012	0.0012
1.6667	0.6667	0.0041	0.0043	0.0044	0.0045	0.0046

Table 3: Numerical solutions of pressure

of the fluid at different times 0.001, 0.002, 0.003, 0.004, 0.005 and x varies from 0.0 to 2.0 and y varies from 0.0 to 1.0 is illustrated in Figures 18 to 22. From these figures for fixed time, either keeping x-fixed or y-varies or keeping y-fixed and x-varies, it has been observed that the pressure increases uniformly. Also for particular values of x and y, it has been observed that the numerical value of pressure increases with the increase in time from t =0.001 to t =0.004. The values of pressure converged thereafter.

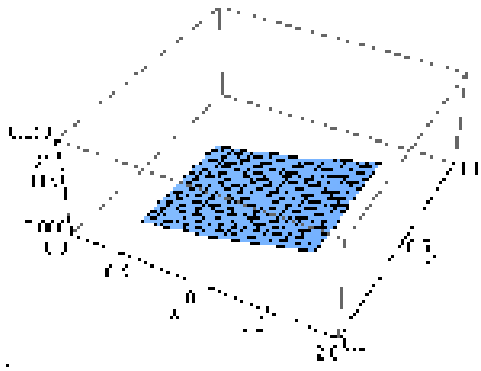

Figure 18: Pressure at t=0.001

The numerical solutions for the temperature at different times 0.001, 0.002, 0.003, 0.004, 0.005 for given values of x and y which varies from 0.0 to 2.0 and 0.0 to 1.0 respectively have been computed and given in Table 3. The temperature of the fluid at different times 0.001, 0.002, 0.003, 0.004, 0.005 and x varies from 0.0 to 2.0 and y varies from 0.0 to 1.0 is illustrated in Figures 23 to 27. From these figures for fixed time, either keeping x-fixed or y-varies or keeping y-fixed and x-varies, it has been observed that the temperature first decreases and then increases uniformly. Also for particular values of x and y,

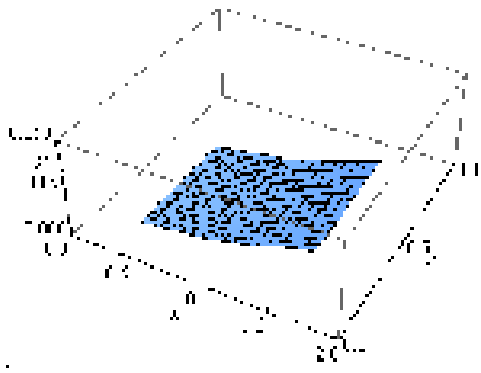

Figure 19: Pressure at t=0.002

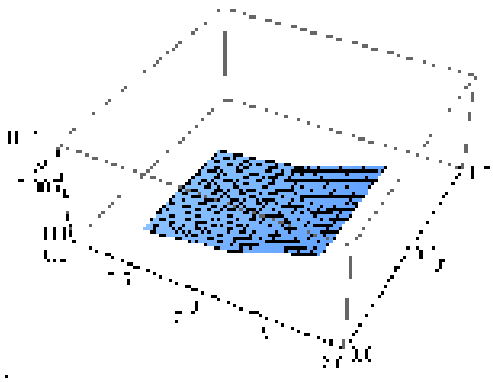

Figure 20: Pressure at t=0.003

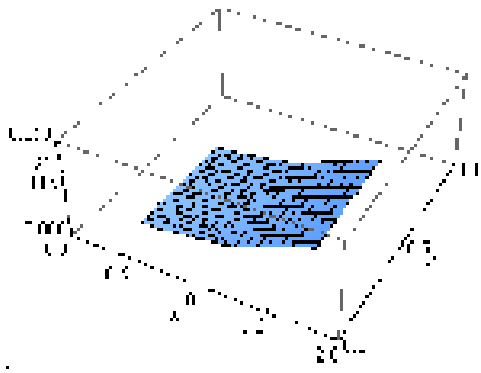

Figure 21: Pressure at t=0.004

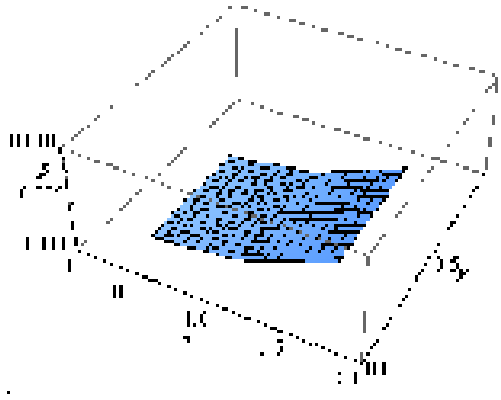

Figure 22: Pressure at t=0.005

x	y	T(t = .001)	T(t = .002)	T(t = .003)	T(t = .004)	T(t = .005)
0.3334	0.1667	0.020178	0.032167	0.036834	0.038153	0.038461
1.0000	0.1667	0.017954	0.026582	0.031082	0.034258	0.034752
1.6667	0.1667	0.020183	0.031437	0.037462	0.039142	0.039583
0.3334	0.3334	0.002337	0.003157	0.003826	0.004103	0.004278
1.0000	0.3334	0.000083	0.000483	0.000516	0.000537	0.000542
1.6667	0.3334	0.002336	0.003154	0.003823	0.004108	0.004273
0.3334	0.6667	0.020189	0.031436	0.037465	0.039145	0.039586
1.0000	0.6667	0.017955	0.026589	0.031086	0.034252	0.034753
1.6667	0.6667	0.020176	0.032164	0.036835	0.038158	0.038464

Table 4: Numerical solutions of temperature

similar behavior can been observed with the increase in time from t =0.001 to t =0.004. The values of temperature converged thereafter.

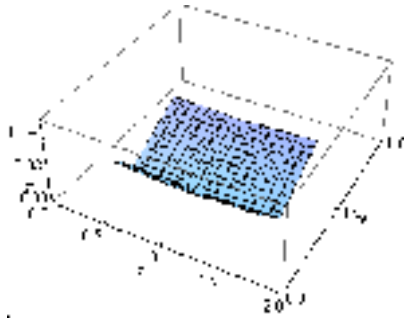

Figure 23: Temperature at t=0.001

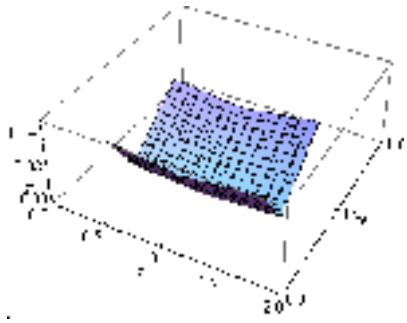

Figure 24: Temperature at t=0.002

6. Conclusions

The problem of an unsteady 2-D incompressible viscous flow with heat transfer at moderate Reynolds number with slip boundary conditions was investigated. Numerical solutions for the governing equations at moderate Reynolds number ($Re = 5000$) obtained using marker and cell (MAC) method. The numerical computations for u-velocity, v-velocity, pressure and temperature were conducted using an efficient solver based on staggered grid system. These numerical computations were performed using a C-programming language. While performing computations for unknown variables like u-velocity, v-velocity, pressure and temperature,$Re = 5000$, $K = 1\Delta t = 0.0005$,$\Delta x = 2/3$,$\Delta y = 1/3$ has been chosen Conclusions of this study are as follows:

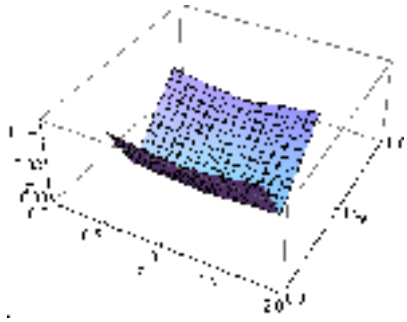

Figure 25: Temperature at t=0.003

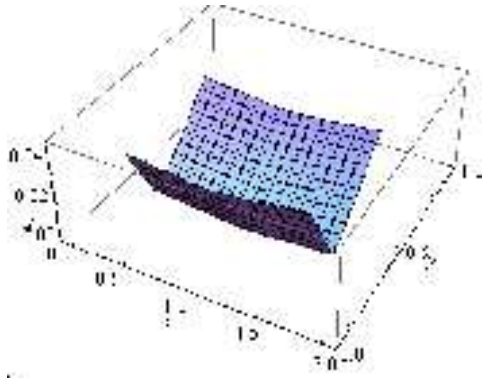

Figure 26: Temperature at t=0.004

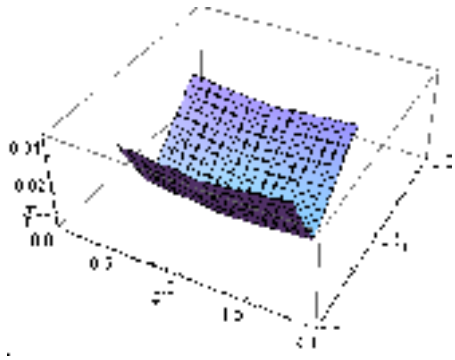

Figure 27: Temperature at t=0.005

1. The u-velocity of the fluid at different times 0.001, 0.002, 0.003, 0.004, 0.005 for different positions (0.6667, 1.3334) along the ox for which y varies from 0.0 to 1.0 has been computed. It can be seen that the u-velocity increases steadily but u-velocity at different time for different positions along x-axis 0.6667, 1.3334 for which the position on y-axis at 0.6667 decreases steadily. In other words we can say that the absolute value of the u-velocity increases as time passes for different positions on oy.

2. The v-velocity of the fluid at different times 0.001, 0.002, 0.003, 0.004, 0.005 for different positions (0.3334, 0.6667) along the oy for which x varies from 0.0 to 2.0 has been computed. It can be seen that for y =0.3334, the v-velocity increases with increase in the value of x. Also at a particular time it has been observed that for y =0.6667, the v-velocity decreases with increase in the value of x.

3. The numerical solutions for the pressure at different times 0.001, 0.002, 0.003, 0.004, 0.005 for given values of x and y which varies from 0.0 to 2.0 and 0.0 to 1.0 respectively have been computed. For fixed time, either keeping x-fixed or y-varies or keeping y-fixed and x-varies, it has been observed that the pressure increases uniformly. Also for particular values of x and y, it has been observed that the numerical value of pressure increases with the increase in time from t =0.001 to t =0.004. The values of pressure converged thereafter.

4. The numerical solutions for the temperature at different times 0.001, 0.002, 0.003, 0.004, 0.005 for given values of x and y which varies from 0.0 to 2.0 and 0.0 to 1.0 respectively have been computed. For fixed time, either keeping x-fixed or y-varies or keeping y-fixed and x-varies, it has been observed that the temperature first decreases and then increases uniformly. Also for particular values of x and y, similar behavior can been observed with the increase in time from t =0.001 to t =0.004. The values of temperature converged thereafter.

Nomenclature

p – Thermodynamic pressure

P – Dimensionless Pressure ($\frac{p}{\rho}$) that has been with respect to ρu^2

Re – Reynolds number, ($^{UL}/_{\nu}$where U and L are characteristic velocity and length and $\nu$is the kinematic viscosity)

K – Diffusivity parameter

T – Temperature

$\mathbf{u}$ – Velocity vector
t – Non-dimensional time
x, y – Co-ordinates
Δx – Grid spacing along x- axis
Δy – Grid spacing along y- axis
Δt – Time spacing
$\nabla \mathbf{u}$ – Divergence of velocity vector
$\nabla \hat{u}$ – Divergence of pseudo-velocity vector
$u = x-$component of the velocity
$\hat{u} = x-$component of the pseudo-velocity
$u^n = x-$component of the velocity after n iterations
$v^n = y-$component of the velocity after n iterations
$v = y-$component of the velocity
$\hat{v} = y-$component of the pseudo-velocity
$\frac{\partial}{\partial n}$ – Differentiation along the normal to the boundary
t^n – Time level after n iterations
Greek symbols
ρ – Fluid density (kg/m^3)
Superscript
n – Pertains to the n iteration
Subscript
i – Index used in tensor notation
j – Index used in tensor notation

Acknowledgments

The authors acknowledge the support from the Council of Scientific and Industrial Research (HRGD, Government of India) for providing research grant under JRF wide letter No. 09/045(0906)/2009-EMR-I to carry out this work.

References

[1] Francis H. Harlow, J. Eddie Welch, Numerical calculation of time dependent viscous incompressible flow of fluid with free surface, *Phys. Fluids*, **8** (1965), 2182-2189.

[2] Suhas V. Patankar, *Numerical Heat Transfer and Fluid Flow*, Hemisphere Publishing Corporation, NewYork (1980).

[3] R. Peyret, T.D. Taylor, *Computational Methods for Fluid Flow*, Springer-Verlag, New York (1983).

[4] Toru Fusegi, Bakitter Farouk, Prediction of fluid flow ad heat transfer problem by the vorticity-velocity formulation of the naive-stokes equations, *Journal of Computational Physics*, **65** (1986), 227-243.

[5] D.A. Kaminiski, X.D. Fu, M.K. Jensen, Numerical and experimental analysis of combine convective and radiative heat transfer in laminar flow over a circular cylinder, *International Journal of Heat Transfer*, **38** (1995), 3161-3169.

[6] D.A. Anderson, R.H. Pletcher, J.C. Tenihill, *Computational Fluid Mechanics and Heat Transfer*, Second Edition, Taylor and Francis, Washington D.C. (1997).

[7] Maksym Grzywinski, Andrzej Sluzalec, Stochastic convective heat transfer equations in finite differences method, *International Journal of Heat and Mass Transfer*, **43** (2000), 4003-4008.

[8] N.T. Eldabe, E.F. Elshehawey, Elsayed M.E. Elbarbary, Nasser S. Elgazery, Chebyshev finite difference method for MHD flow of a micro polar fluid past a stretching sheet with heat transfer, *Applied Mathematics and Computation*, **160** (2005), 437-450.

[9] Arnab Kumar De, Amaresh Dalal, A numerical study of natural convection around a square, horizontal, heated cylinder placed in an enclosure, *International Journal of Heat and Mass Transfer*, **49** (2006), 4608–4623

[10] P.H. Chiu, Tony W.H. Sheu, R.K. Lin, An effective explicit pressure gradient scheme implemented in the two-level non-staggered grids for incompressible Navier–Stokes equations, *Journal of Computational Physics*, **227** (2008), 4018-4037.

[11] H.K. Versteeg, W. Malalsekra, *An Introduction to Computational Fluid Dynamics: The Finite Volume Method*, Second Edition, Pearson, India (2007).

[12] Tomasz Piasecki, Steady compressible Navier-Stokes flow in a square, *Journal of Mathematical Analysis and Applications*, **357** (2009), 447-467.

[13] Qiaolin He, Xiao-Ping Wang, Numerical study of the effect of Navier slip on the driven cavity flow, *ZAMM Z. Angew. Math. Mech.*, **89** (2009), 857-868.

[14] A.A. Lambert, S. Cuevas, J.A. del Rio, M. Lopez de Haro, Heat transfer enhancement in oscillatory flows of Newtonian and viscoelastic fluids, *International Journal of Heat and Mass Transfer*, **52** (2009), 5472-5478.

[15] Saleh M. Alharbi, Mohamed A.A. Bazid, Mahmoud S. El Gendy, Heat and mass transfer in MHD visco-elastic fluid flow through a porous medium over a stretching sheet with chemical reaction, *Applied Mathematics*, **1** (2010), 446-455.

[16] Sedat Biringen, Chuen-Yen Chow, *An Introduction to Computational Fluid Mechanics by Example*, John Wiley and Sons, New Jersey (2011).

[17] Tiegang Fang, ShanshanYao, Ioan Pop, Flow and heat transfer over a generalized stretching/shrinking Wall problem – Exact solutions of the Navier-Stokes equations, *International Journal of Non-Linear Mechanics*, **46** (2011), 1116–1127.

[18] B.H. Salman, H.A. Mohammed, A. Sh. Kherbeet, Heat transfer enhancement of nanofluids flow in microtube with constant heat flux, *International Communications in Heat and Mass Transfer*, **39** (2012), 1195-1204.

[19] Asma Begum, Md. Abdul Maleque, M. Ferdows, Masahiro Ota, Finite difference solution of natural convection flow over a heated plate with different inclination and stability analysis, *Applied Mathematical Sciences*, **6** (2012), 3367-3379.

[20] M. Hasanuzzaman, M.M. Rahman, Hakan F. Oztop, N.A. Rahim R. Saidur, Effects of Lewis number on heat and mass transfer in a triangular cavity, *International Communications in Heat and Mass Transfer*, **39** (2012), 1213-1219.